The Effect of Certain Processing Variables on the Form II to Form I Phase Transformation in Polybutene-1

KWANG-BUM HONG and JOSEPH E. SPRUIELL, *Polymer Engineering, University of Tennessee, Knoxville, Tennessee 37996-2200*

Synopsis

Density and wide angle x-ray scattering techniques were used to study the form II to form I phase transformation in polybutene-1. The influence of deformation by cold rolling, orientation produced by melt processing (film blowing), and certain additives blended with the homopolymer on the phase transformation behavior were examined. A new technique based on a combination of wide angle X-ray diffraction and density measurements was devised to determine the relative fractions of form I, form II, and amorphous phases present. Small reductions in thickness by cold rolling cause a rapid partial transformation to form I followed by further transformation at enhanced rates. The enhancement of crystal transformation by cold rolling is primarily the result of the stresses or strains applied rather than the orientation produced. The introduction of molecular orientation by melt processing also enhances the rate of the form II to form I phase transformation, but it is rather less effective than small amounts of cold rolling which themselves produce comparatively little change in molecular orientation. The mechanical blending of polypropylene with polybutene-1 was found to accelerate the form II to form I phase transformation, while another additive (1-naphtylacetamide) known to be a good nucleating agent for crystallization of polybutene-1 did not increase the rate of phase transformation when added at concentration levels needed to nucleate crystallization from the melt.

INTRODUCTION

Since its synthesis and initial characterization by Natta and co-workers,[1,2] isotactic polybutene-1 has attracted considerable attention due to its excellent physical properties and its unusual polymorphic phase transitions.

The polymorphs of isotactic polybutene-1 have been investigated by many authors.[3-5] There exist at least five different crystal structures involving three helical conformations. It is well known that among these crystal structures, the tetragonal crystal modification (form II) forms from the melt and then transforms slowly into the hexagonal crystal modification (form I) resulting in changes of mechanical, thermal, and physical properties.[3] This crystal transformation is known to be affected by elapsed time, temperature, and mechanical deformation.[3,6-12]

A major drawback of polybutene-1 is its slow crystallization kinetics (compared to other polyolefins such as polyethylene and isotactic polypropylene).[3,10,13] This combined with the form II to form I phase transformation, which may require several days for completion, makes polybutene-1 complicated and slow to process. Because of its significance with respect to the processing of polybutene-1, methods for the acceleration of both crystallization and transformation have been broadly investigated. These studies

Journal of Applied Polymer Science, Vol. 30, 3163–3188 (1985)
 CCC 0021-8995/85/083163-26$04.00

have included investigation of the ability of nucleating agents to enhance crystallization kinetics from the melt[14-16] and various means to enhance the phase transformation including high atmospheric pressure[17] and extensional solid state deformation,[6,7,9,11,12,18] and even the copolymerization of butene-1 monomer with some traditional olefins such as ethylene, propylene, etc.[19] However, it was also found that this transformation could be retarded by copolymerizing the butene-1 monomer with linear α-olefins ($c > 5$) and the branched comonomers,[19] or by keeping the polybutene-1 samples at certain aging temperatures.[3,12,18]

There seem to be no studies dealing with cold rolling per se as a method of enhancing the phase transformation rate. Among the solid state deformation processes, rolling would appear to hold promise for improving the mechanical properties while accelerating the formation of the stable form I phase. One of the goals of the present paper was to investigate the effect that room temperature rolling has on the phase transformation kinetics. The question of the effects of rolling on the mechanical properties is described in a companion paper.[20]

The effect of molecular orientation produced by melt processing has also received little prior attention. A second goal of the present work was to examine the effect of molecular orientation produced by the tubular film blowing process on the subsequent form II to form I phase transformation rate.

Finally, it has been suggested[21] that certain agents blended with polybutene-1 have a substantial effect on the phase transformation. We also describe here a study of certain selected additives.

During these studies we have found it useful to develop a new technique for monitoring the progress of the phase transformation. By combining measurements of the density of selected standard samples with wide angle X-ray diffraction measurement of crystal peak intensities, it was possible to determine the approximate fractions of form I, form II, and amorphous phases present in a given sample. Previous studies have generally followed the progress of the phase transformation by evaluating the relative fraction of form I crystal in the total amount of crystalline material without regard for an observed change in total crystallinity during the transformation.[11,22] The new technique lets us clearly observe these changes with time.

MATERIALS AND EXPERIMENTAL PROCEDURES

Materials

The primary material investigated in this study was a commercial polybutene-1 called BR 200S resin supplied by Shell Development Company and having the characteristics given in Table I. BR 200S is a homopolymer resin containing a small amount of stabilizer. A second commercial resin,

TABLE I
Polybutene-1 Used

	Company	Melt index	M_w	M_w/M_n	Density
PB-1 BR200S	Shell	0.4	700,000	10	0.915
PB-1 DP1710SA	Shell	1.0		>17	0.910

TABLE II
Composition, Code Numbers and DSC Crystallization Temperatures[a] for Additive Containing Polybutene-1 Samples

Samples	Code numbers	Onset temp (°C)	Peak Temp (°C)
Polybutene-1 BR resin (homopolymer)	PBN0	62.8	56.2
0.1% sodium benzoate + BR resin	PBN1	63.5	57.3
0.5% sodium benzoate + BR resin	PBN2	61.0	52.7
5% polypropylene + BR resin	PBN3	72.7	68.7
10% polypropylene + BR resin	PBN4	73.0	69.1
0.1% (1-naphtylacetamide) + BR resin	PBN6	66.7	57.7
0.5% (1-naphtylacetamide) + BR resin	PBN7	78.3	68.0
0.1% stearic acid + BR resin	PBN8	63.7	56.1
0.5% stearic acid + BR resin	PBN9	64.2	57.7

[a]All samples cooled at 40°C/min from 180°C.

DP 1710SA, was also studied briefly for comparison to BR 200S. The DP 1710SA resin is a film grade which is modified in some proprietary manner to achieve better processing characteristics for film production.

Samples of the BR resin containing various additives were also prepared. The compositions of these samples are given with their code numbers in Table II. The compositions are weight percent based on the weights of the ingredients.

The polypropylene used as an additive was Hercules Profax 6823 (MI = 0.33). The other additives used are sodium benzoate, 1-naphtylacetamide, and stearic acid. These compounds are known to be effective as nucleating agents for polyolefin crystallization from the melt.[14,15,16,23] These materials were added in the form of fine powders.

The preparation of the additive containing samples was carried out by using a Brabender extruder connected to a Koch static mixer. Mechanical mixtures of polybutene-1 and additive were first extruded through this combination at an extrusion temperature of 180°C. The mixed and solidified extrudates were cut into pellets for subsequent reprocessing. Samples PBN1-PBN4 were prepared from master batches containing higher concentrations. The master batches were diluted by a second mixing with polybutene-1 homopolymer and extrusion through the static mixer.

Tubular Film Extrusion

The polybutene-1 tubular blown films were produced with a 0.75 in. Rainville screw extruder with an annular blown film die (inside diameter = 1.396 cm and outside diameter = 1.605 cm). The extrusion temperature was 180°C. A series of three films were prepared for each of the two resins. The conditions of preparation are shown in Table III.

Compression Molding and Cold Rolling

Pellets of the polybutene-1 samples were compression molded between two preheated platens at 230°C. The pellets were preheated without pressure for about 30 min, and then the pressure was applied for a few minutes. The pressure was applied and released repeatedly during the compression molding. The sample was then removed from the press and quenched by

TABLE III
Summary of Polybutene-1 Films Prepared

Sample	Blowup ratio	Drawdown ratio V_L/V_0	Film thickness (μm)
1 (BR resin)	1	1	390
2 (BR resin)	1	3	110
3 (BR resin)	1	6	55
4 (DP resin)	1	1	370
5 (DP resin)	1	3	125
6 (DP resin)	1	6	75

plunging it into an ice water bath. The time at which the sample was quenched was taken as the origin of aging time for fresh samples. The thickness of the sheets was about 1,000 μm (1 mm).

Billets of polybutene-1 were cut from the compression-molded sheets. These were rolled to various thicknesses at room temperature using a rolling mill with 100 mm diameter steel rolls. The reduction in thickness through the rolls was in general from 0.05 to 0.10 mm per pass. To ensure uniformity in rolling conditions, sheets were reversed end for end and turned bottom side up after each pass. In the present experiments, the compression-molded sheets were rolled only at room temperature (25°C). The amount of cold rolling was assumed equal to the thickness reduction and was calculated by the following:

$$\text{thickness reduction (\%)} = \frac{t_0 - t}{t_0} \times 100 \tag{1}$$

where t_0 is the original thickness of a billet before rolling and t is the thickness of the rolled billet.

Density Measurement by Density Gradient Column

In order to determine the initial and final crystallinities, and the time-dependent densities of polybutene-1, a water–isopropyl alcohol density gradient column was used. It was necessary to cut the samples large enough to promote settling in order to obtain meaningful measurements at short aging times.

Wide Angle X-Ray Diffraction Measurements

Tubular blown films or compression-molded sheets (unrolled or rolled) were immediately cut into a rectangular shape and attached to the sample holder of a Rigaku X-ray diffractometer. The diffractometer was controlled by a microprocessor which could be programmed to measure the integral diffraction intensity corrected for background from any chosen crystalline plane.

The degree of crystal transformation, ϕ, defined as the volume fraction of form I crystal in the total crystal, was measured using the method of Oda et al.[12] This method involves measurement of the intensity of the

crystalline reflections in the angular range 8–30°, 2θ. The degree of crystal transformation is then given by

$$\phi = \frac{I_{110(I)} + I_{300(I)} + I_{220/211(I)}}{I_{110(I)} + I_{200(II)} + I_{220(II)} + I_{300(I)} + I_{213(II)} + I_{220/211(I)}} \tag{2}$$

$I_{hkl}(i)$ is the integral diffraction intensity from each crystal plane, hkl represents the Miller index of the crystal plane, and (i) designates the crystal of form I or form II. The degree of crystal transformation, ϕ, may then be plotted against aging time after preparation.

Although ϕ vs. time plots give a measure of the rate of transformation from crystal form II to crystal form I, ϕ does not give an indication of the total crystallinity in the sample. In order to obtain a measure of the fraction of form I, form II, and amorphous phases present in the samples as a function of aging time, it was necessary to develop a new method of phase analysis based on a combination of density and X-ray diffraction techniques.

The new method utilizes two "standard samples." One of these, the extreme crystal form I standard, is high in the form I content but contains negligible form II content while the extreme crystal form II standard, is high in the form II content but has negligible form I content. The crystallinities of each extreme standard sample were calculated from density data through the equation

$$X = \frac{\rho_c}{\rho} \cdot \frac{(\rho - \rho_a)}{(\rho_c - \rho_a)} \tag{3}$$

In the case of crystal form I the theoretical crystal density ρ_c, was calculated to be 0.95 g/cm^3. Form II has the theoretical crystal density of 0.90 g/cm^3. The amorphous density ρ_a, was obtained by linear extrapolation to 23° C of values measured in a range of temperatures above the melting point. The resulting value was $\rho_a = 0.870$ g/cm^3, which is in fair agreement with values in the literature.[1,10]

The ratio R is defined as the ratio of the integrated intensity of the crystal form I peaks only to the integrated intensity of the total scan except the incoherent (background) scattering in the range of 5–30°, 2θ. Similarly, the ratio Q is defined as the ratio of the intensity of the crystal form II peaks only to the total intensity I_t, corrected for background scattering I_b, in the range of 5–30°, 2θ:

$$R = \frac{I_{\mathrm{I}}}{I_{\mathrm{I}} + I_{\mathrm{II}} + I_{\mathrm{am}}} = \frac{I_{\mathrm{I}}}{I_{\mathrm{cry}} + I_{\mathrm{am}}} = \frac{I_{\mathrm{I}}}{I_t - I_b} \tag{4}$$

$$Q = \frac{I_{\mathrm{II}}}{I_{\mathrm{I}} + I_{\mathrm{II}} + I_{\mathrm{am}}} = \frac{I_{\mathrm{II}}}{I_{\mathrm{cry}} + I_{\mathrm{am}}} = \frac{I_{\mathrm{II}}}{I_t - I_b} \tag{5}$$

For an arbitrary sample, we may define "form I index" X_I, the approximate mass fraction of the sample, which is crystal form I phase, as

$$X_{\mathrm{I}} = \frac{R}{R_{\mathrm{I}}^S} \cdot X_{\mathrm{I}}^S \tag{6}$$

"Form II index" X_{II} similarly can be defined as

$$X_{II} = \frac{Q}{Q_{II}^S} \cdot X_{II}^S \tag{7}$$

where X_I^S and X_{II}^S are the crystallinities of two extreme standards which can be calculated from density measurements. R_I^S and Q_{II}^S are the appropriate values of R and Q for the two extreme standards. Note that $X_I + X_{II} + X_{am} = 1$. Also notice that the technique does not require density measurements on any samples except the two extreme standards.

All wide angle X-ray diffraction measurements were made using crystal monochromated CuKα radiation with a wavelength of 1.542 Å. The samples were rotated in the plane of the film during measurement in order to help eliminate any effects due to orientation.

Small Angle Light Scattering

The superstructures of the blown films were investigated by making H_v and V_v small angle light scattering patterns. The patterns were recorded on polaroid film using an He–Ne laser beam of wavelength 6328 Å. The apparatus and technique are similar to that described previously.[24]

The H_v light scattering patterns were analyzed according to the method described by Hashimoto et al.[25] to obtain two shape parameters of the "sheaf-like or fan-like superstructure." One of the shape parameters, γ, measures the angular spread of the "fan" model while the other parameter measures the radius R of the "fan-like superstructures."

EXPERIMENTAL RESULTS

Characteristics of the Transformation in Compression Molded and Lightly Cold Rolled Sheets

The degree of transformation, ϕ, measured by X-ray diffraction through eq. (2) is shown plotted in Figure 1 for the compression molded and lightly

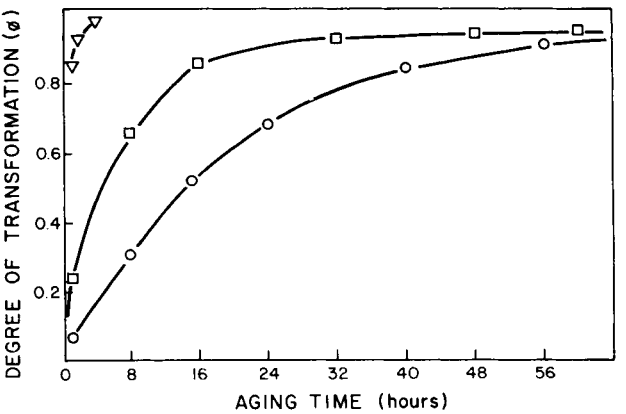

Fig. 1. (▽) 10% cold rolling; (□) 5% cold rolling; (○) no cold rolling. T = 23°C.

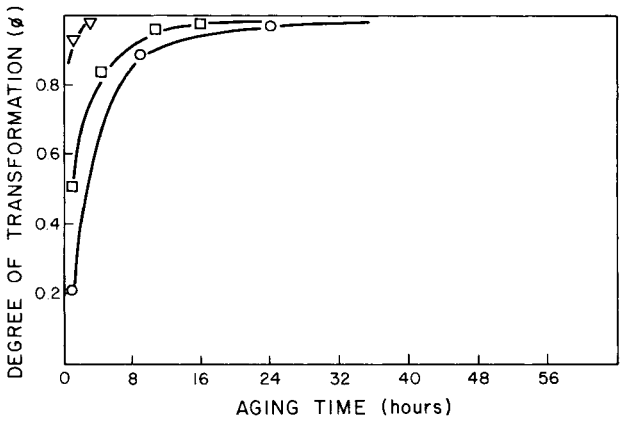

Fig. 2. (▽) 8% coldrolling; (□) 5% cold rolling; (○) no cold rolling. $T = 23°C$.

cold rolled BR resin. Similar results for the DP resin are shown in Figure 2. Comparing the as-compression molded results (no cold rolling) in Figures 1 and 2, we note that the transformation rate in the DP resin is much faster than in the BR (homopolymer) resin. Cold rolling greatly accelerates the transformation in both resins. The transformation is essentially completed within four hours for samples reduced 10% in thickness by cold rolling. Higher reductions resulted in the transformation reaching completion too fast to be readily measurable by the technique used in this research.

In Figure 3 wide angle X-ray scattering patterns of as-compression molded and lightly cold rolled BR resin samples are presented. It can be seen that even the 20% cold rolled samples show little evidence of any preferred orientation. Determination of pole figures for cold rolled polybutene-1 samples further established that appreciable orientation does not develop until more than 20% cold reduction is taken. This suggests that the main driving force for the acceleration of the crystal transformation of the cold rolled samples is not orientation but the stresses or strains applied. This suggestion is further supported by the results to be presented below for oriented sam-

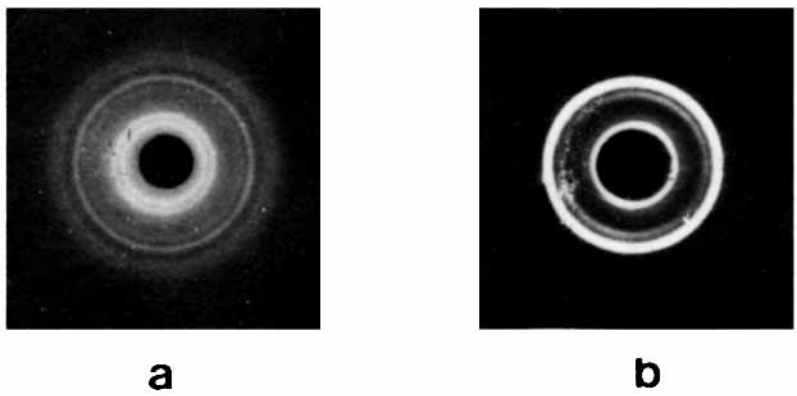

Fig. 3. Wide angle patterns of compression molded and cold rolled polybutene-1: (a) two-phase structure of compression molded and slightly aged sample; (b) form I pattern of 20% cold reduced sample.

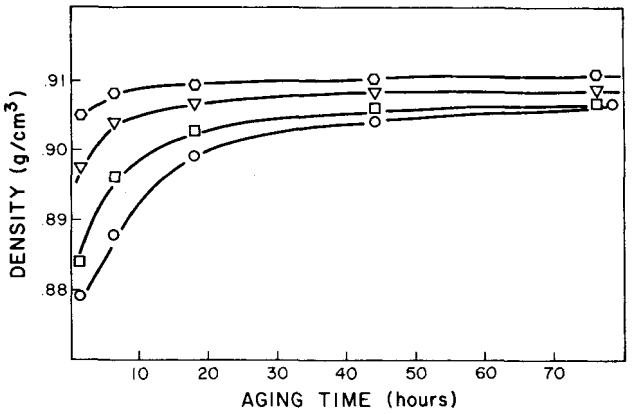

Fig. 4. (○) 20% cold rolling; (▽ 10% cold rolling; (□) 5% cold rolling; (○) no cold rolling. $T = 23°C$.

ples produced by the tubular film blowing technique. Although such orientation has an effect on the rate of the crystal transformation, it is not as great as the effect of small reductions by cold rolling.

As shown in Figures 4 and 5, the density of PB-1 increases during the crystal transformation. In fact, this was expected because the density of either crystal form is greater than that of amorphous supercooled melt and the density of crystal form I is greater than that of crystal form II. Thus the density of polybutene-1 increases both with crystallinity and crystal transformation. However, in the absence of the relative amounts of form II and form I determined by some other method, it is impossible to separate the contribution of crystallinity and crystal transformation to the change of density. The new method of computing crystallinity indexes for both phases was developed to allow this separation. This will be described in more detail later.

The sharp increase of initial density (ρ_0) according to the degree of deformation is interpreted to indicate that there is an increase of the initial degree of crystal transformation (ϕ_0) with increase in the deformation.

It is interesting to note that the large differences between initial densities of unrolled and cold rolled samples get smaller and smaller with increasing

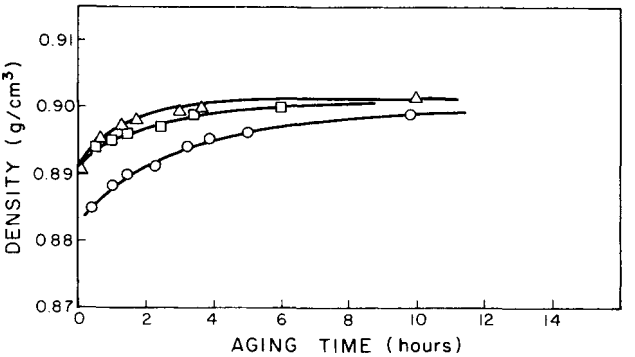

Fig. 5. (△) 8% cold rolling; (□) 5% cold rolling; (○) no cold rolling. $T = 23°C$.

aging time. These differences disappear rapidly for the DP resin. This suggests that, given enough time, all samples approach the same equilibrium density value for transformation at room temperature.

The standard sample densities of polybutene-1 were combined with the intensity data in order to calculate the "crystallinity indexes" of the two crystal forms, i.e., X_{I} and X_{II}. The total crystallinity, X_T, was the simple addition of these two "crystallinity indexes." A major advantage of this new phase analysis method is that once the results for two standard samples of polybutene-1 are established, they can be used throughout the whole of the experiments to calculate the "crystallinity indexes" of any other polybutene-1 samples from only their X-ray intensity data.

Typical results for the technique are shown in Figure 6 for the as-compression molded BR resin. Results for this sample are also given in Table IV along with results for 5% and the 10% cold rolled BR resin and the 0, 5, and 8% cold rolled DP resin.

The experimental density data of Figures 4 and 5 can also be used to provide a check on the validity of the new method of phase analysis. This was done by comparing the experimental density measured in the density gradient column with the density of the X-ray samples calculated by the following equation:

$$\bar{V} = \bar{V}_{\mathrm{I}}X_{\mathrm{I}} + \bar{V}_{\mathrm{II}}X_{\mathrm{II}} + \bar{V}_{\mathrm{am}}X_{\mathrm{am}} \tag{8}$$

The values of the X_{I}, X_{II}, and X_{am} were obtained from the new X-ray diffraction phase analysis technique while the $\bar{V}_{\mathrm{I}}$, $\bar{V}_{\mathrm{II}}$, and $\bar{V}_{\mathrm{am}}$ are the theoretical specific volumes of form I and form II, and the amorphous specific volume, respectively. The results of this comparison are shown in the last two columns of Table IV. The calculated and experimental densities agree within the anticipated experimental error.

As shown in Figure 6 for the undeformed BR resin and in Figure 7 for the undeformed DP resin, the amount of form II gradually decreases from its initial value while the amount of form I gradually increases. The rate of this change is much greater for the DP resin than for the BR resin as expected. The total crystallinity of as-compression molded BR resin is about 0.30–0.35 at the earliest measurement that can be made. It is assumed that the bulk of this value is developed by crystallization to form II during and immediately following the quenching process as suggested by previous investigators.[3,10]

The level of crystallinity of compression molded samples increases at first at a rate that depends on the type of resin, but it seems to approach an asymptotic value after a few days.

The form I crystalline fraction is plotted as a function of time in Figures 8 and 9. It can be seen that cold work produces an abrupt increase in form I at short transformation times. This is consistent with the density data of Figures 4 and 5. The increase of initial density is largely associated with a large increase in form I material resulting from the cold work. The high initial fractions of form I are accompanied by a reduction in the amount of form II that is present. In fact, the sharp decrease of X_{II} in the deformed samples (e.g., BR 10% and DP 8% in Table IV) further attests to the large

TABLE IV
Time Dependence of Crystallinity and Density of Compression Molded and Cold Rolled BR Resin

Time T	Form II fraction	Form I fraction	Crystalline fraction	Amorphous fraction	Exptr density (g/cm^3)	Calcd density (g/cm^3)
Sample: BR 0% cold rolled						
1 h	0.333	0.020	0.353	0.647	0.879	0.881
2 h	0.321	0.038	0.359	0.641	0.882	0.882
3 h	0.304	0.054	0.358	0.642	0.884	0.883
15 h	0.182	0.269	0.451	0.549	0.897	0.896
19 h	0.154	0.317	0.471	0.529	0.899	0.899
45 h	0.054	0.453	0.507	0.493	0.904	0.906
91 h	0.032	0.496	0.528	0.472	0.906	0.908
Final	0.017	0.520	0.537	0.463	0.910	0.910
Sample: BR 5% cold rolled						
10 min	0.253	0.043	0.296	0.704	0.880	0.881
70 min	0.251	0.104	0.355	0.645	0.884	0.885
200 min	0.144	0.200	0.344	0.656	0.891	0.889
15 h	0.063	0.428	0.491	0.509	0.901	0.904
19 h	0.050	0.458	0.508	0.492	0.903	0.906
44 h	0.025	0.474	0.499	0.501	0.906	0.907
67 h	0.027	0.537	0.564	0.436	0.907	0.912
Sample: BR 10% cold rolled						
20 min	0.018	0.396	0.414	0.586	0.902	0.901
60 min	0.013	0.422	0.435	0.565	0.906	0.902
90 min	0.013	0.397	0.410	0.590	0.906	0.901
120 min	0.010	0.404	0.414	0.586	0.906	0.901
150 min	0.007	0.413	0.420	0.580	0.907	0.902
45 h	0.003	0.476	0.479	0.521	0.910	0.906
Sample: DP 0% cold rolled						
25 min	0.201	0.106	0.307	0.693	0.885	0.884
60 min	0.153	0.139	0.292	0.708	0.888	0.885
90 min	0.146	0.170	0.316	0.684	0.889	0.887
135 min	0.123	0.216	0.339	0.661	0.891	0.890
190 min	0.097	0.291	0.388	0.612	0.894	0.895
230 min	0.078	0.325	0.403	0.597	0.895	0.897
Sample: DP 5% cold rolled						
30 min	0.162	0.108	0.270	0.730	0.894	0.883
60 min	0.138	0.165	0.303	0.697	0.895	0.886
90 min	0.120	0.192	0.312	0.688	0.896	0.888
150 min	0.088	0.254	0.342	0.658	0.897	0.892
205 min	0.062	0.293	0.355	0.645	0.899	0.894
6 h	0.037	0.378	0.415	0.585	0.900	0.900
Sample: DP 8% cold rolled						
10 min	0.021	0.349	0.370	0.630	0.890	0.897
40 min	0.015	0.379	0.394	0.606	0.895	0.899
80 min	0.009	0.389	0.398	0.602	0.897	0.900
105 min	0.013	0.391	0.404	0.596	0.898	0.900
180 min	0.006	0.417	0.423	0.577	0.899	0.902
220 min	0.005	0.434	0.439	0.561	0.900	0.903

effect of deformation in enhancing the crystal transformation of these samples.

If there is no secondary crystallization from the supercooled melt, the total crystallinity, X_T, should be constant during the crystal transformation.

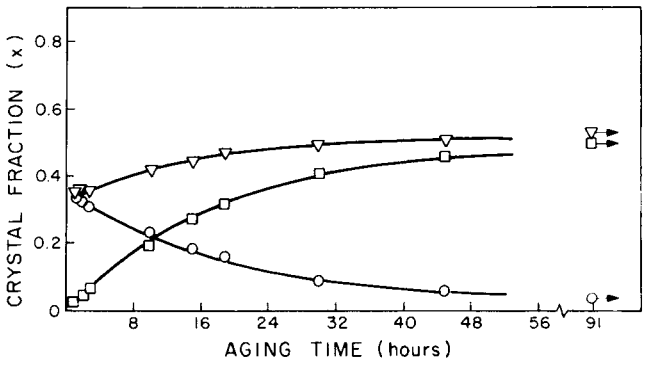

Fig. 6. (▽) x_T; (□) x_I; (○) x_{II}. $T = 23°C$.

This assumes that the crystal transformation phenomenon itself does not involve any increment of crystallinity. However, the total crystallinity actually increases during the crystal transformation, as shown in Figures 6 and 7, and the amount of form I present eventually exceeds the initial degree of total crystallinity. This means that secondary crystallization takes place with the crystal transformation. The time origin of the secondary crystallization is assumed to be around the beginning of the crystal transformation (0 aging time). However, the exact origin of the secondary crystallization cannot be determined at this point due to lack of sufficient experimental data. It is noteworthy that the rate of the secondary crystallization is greater in the DP resin than in the BR resin.

The Effect of Melt Processing on the Form II to Form I Crystal Transformation

It is now well established that stretching and other forms of deformation in the solid state accelerate the crystal-crystal phase transformation in polybutene-1.[6,7,9,11,12,18] However, little is known about the effect of melt deformation and the orientation that results from processing operations such as melt spinning and tubular film blowing. We describe here the results of studies of tubular film blowing.

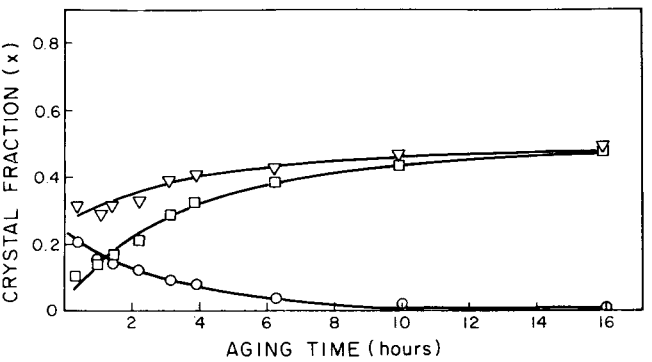

Fig. 7. (▽) X_T; (□) X_I; (○) X_{II}. $T = 23°C$.

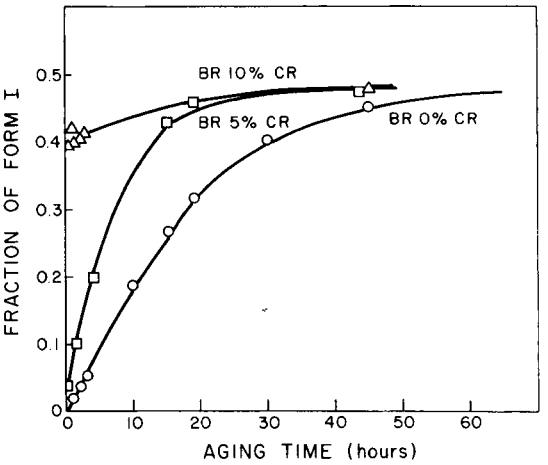

Fig. 8. Fraction of form I vs. aging time. $T = 23°C$.

Because of the relatively slow crystallization kinetics of polybutene-1 and the soft nature of the crystal form II, it is difficult to blow films from unmodified polybutene-1 homopolymer (BR resin). With care it was possible to produce a series of samples with different drawdown ratios (DDR) while maintaining blowup ratio constant at unity; i.e., BUR = 1. Here DDR is the ratio of the takeup velocity to the extrusion velocity and BUR is the ratio of the final bubble diameter to the diameter of the annular film die.

Substantial molecular orientation is produced in the blown films, especially at the higher drawdown ratios. This is readily detected by x-ray diffraction (Fig. 10) and birefringence measurements (Table V) carried out on samples that have been aged to allow transformation to form I. Both the X-ray patterns of Figure 10 and the birefringence measurements in Table V indicate that the level of orientation increases with DDR and is very similar in the BR and DP resins. The orientation becomes more nearly uniaxial in nature as the drawdown ratio increases. (For the ideal uniaxial case $\Delta n_{12} = \Delta n_{13}$ and $\Delta n_{23} = 0$. Here the subscript 1 represents the machine

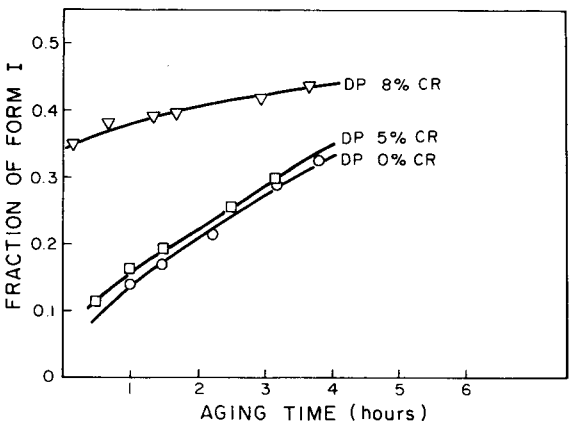

Fig. 9. Fraction of form I vs. aging time $T = 23°C$.

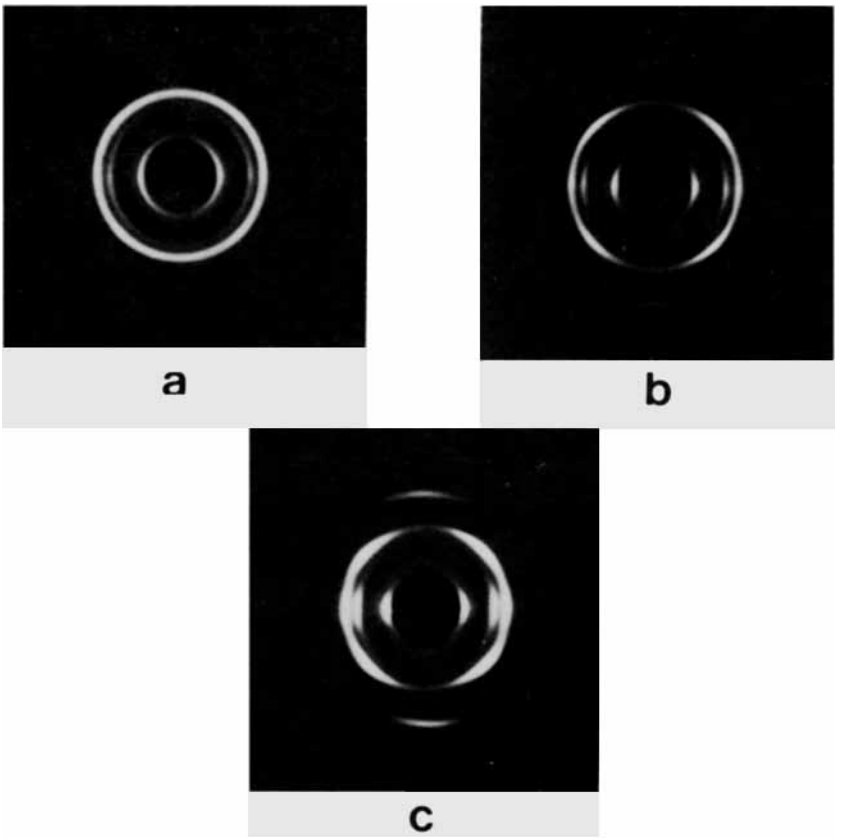

Fig. 10. Wide angle X-ray diffraction patterns of tubular blown films: (a) BR resin, DDR = 1; (b) BR resin, DDR = 3; (c) BR resin, DDR = 6.

direction, 2 the transverse direction, and 3 the direction normal to the film plane.)

In addition to molecular orientation, melt deformation is known to produce other effects in polybutene-1 and other polyolefins. The molecular orientation produced in the melt by deformation substantially increases the crystallization rate and changes the morphology of crystallization.[13,24-27]

TABLE V
Birefringence Data of Tubular Blown Films of Polybutene-1

	BR	DP
DDR = 1	$\Delta n_{12} = 0.68 \times 10^{-3}$	$\Delta n_{12} = 0.74 \times 10^{-3}$
	$\Delta n_{23} = -0.35 \times 10^{-3}$	$\Delta n_{23} = -0.28 \times 10^{-3}$
	$\Delta n_{13} = 0.33 \times 10^{-3}$	$\Delta n_{13} = 0.46 \times 10^{-3}$
DDR = 3	$\Delta n_{12} = 8.43 \times 10^{-3}$	$\Delta n_{12} = 7.49 \times 10^{-3}$
	$\Delta n_{23} = -1.10 \times 10^{-3}$	$\Delta n_{23} = -1.38 \times 10^{-3}$
	$\Delta n_{13} = 7.33 \times 10^{-3}$	$\Delta n_{13} = 6.11 \times 10^{-3}$
DDR = 6	$\Delta n_{12} = 16.33 \times 10^{-3}$	$\Delta n_{12} = 18.41 \times 10^{-3}$
	$\Delta n_{23} = -0.51 \times 10^{-3}$	$\Delta n_{23} = -0.74 \times 10^{-3}$
	$\Delta n_{13} = 15.82 \times 10^{-3}$	$\Delta n_{13} = 17.67 \times 10^{-3}$

Although we did not measure the crystallization kinetics for our samples, we assume that the melt deformation leads to the oriented, accelerated crystallization of crystal form II which eventually transforms into the oriented crystal form I. The change in crystalline morphology due to melt processing was demonstrated using small angle light scattering (SALS). The SALS patterns for our blown films were similar to those described by Hashimoto et al.[25] and they were interpreted to indicate "sheaflike" or distorted spherulite structures. According to the "fan model" of Hashimoto et al., this morphology can be characterized in terms of two shape parameters; namely, the aperture angle 2γ and the radius R of the "fan model." When the aperture angle is 180°, the superstructure can be interpreted as a spherulite.

The shape parameters of our tubular blown films calculated according to the method of Hashimoto et al.[25] are presented in Table VI. The morphology changes from almost spherulitic at DDR = 1 to "sheaflike" structure ($\gamma < 90°$) with increased drawdown of the polymer melt. The size of superstructure also decreases as the drawdown ratio increases. It is important to note that the measurements were made on samples that had already transformed to form I. However, it is unlikely that the morphology at the superstructure level changes appreciably during the phase transformation.[10,25,28]

In Figure 11 it is confirmed that the changes in orientation and morphology produced by changes in melt processing procedures effect changes in the form II to form I transformation rate. Increasing the drawdown ratio increases the crystal transformation rate. Blown films produced with the lowest drawdown (DDR = 1) transform at a rate that is somewhat greater than that of the as-compression molded samples; compare Figures 11 and 1. Data for the DP resin show that it transforms faster than the BR resin, but the enhancement caused by melt orientation is similar in nature. It should be noted that the film thickness changed with increase of DDR. Some previous investigators[3,29] have suggested that thickness changes alone can lead to changes in transformation rate. It is believed that, in the range of thicknesses studied here, this effect will not be significant.

The new method of phase analysis was also applied to the blown film samples. In general, the results confirmed that increasing the DDR enhanced the rate of change of both form I and form II. The results further showed that higher drawdown ratios also lead to higher total crystallinities at any specified aging time up to several hours (Table VII). High drawdown

TABLE VI
Superstructure Shape Parameters for Polybutene-1 Blown Films

	μ_{max} (°)	θ_{max} (°)	γ (°)	R (μm)
BR DDR = 1	45	2.78	75–90	8.31
BR DDR = 3	21	8.18	25	4.18
BR DDR = 6	25	11.48	32	2.63
DP DDR = 1	45	3.57	75–90	6.49
DP DDR = 3	25	8.18	32	3.89
DP DDR = 6	30	10.62	40	2.57

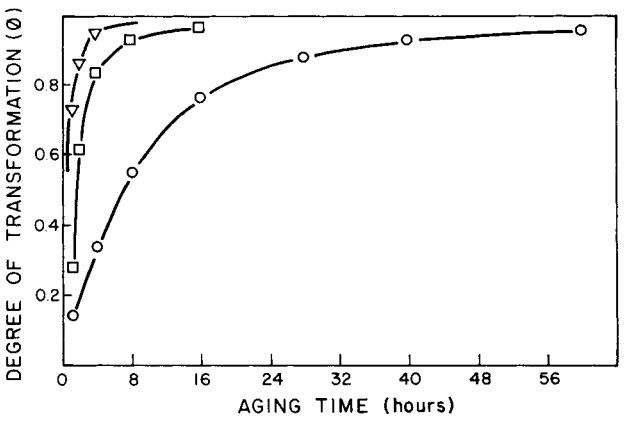

Fig. 11. (▽) DDR = 6, t = 55 μm; (□) DDR = 3, t = 110 μm; (○) DDR = 1, t 390 μm. BUR = 1, T = 23°C.

ratio also produces total crystallinities higher than those found in compression molded and aged samples. The bulk of initial crystallinity of these samples must come from the crystallization from the melt during and immediately following the quenching process of these samples. Table VII shows that the initial crystalline form I fraction increases sharply by increasing the drawdown ratio while the initial fraction of form II does not appear very sensitive to drawdown ratio. It is interesting to note that the increment of X_I (ΔX_I) is almost always greater than that of X_{II} (ΔX_{II}) for a given time, as may be confirmed from Table VII. This, of course, results in the gradual increase in total crystallinity. There are two possible explanations for these observations. One is the additional crystallization of form II from the supercooled melt with increasing DDR coupled with a rapid transformation to form I. Another possible mechanism is the direct crystallization of form I from the supercooled melt. Since both of these two mechanisms could possibly lead to increased early values of X_I coupled with the fact that $\Delta X_I > \Delta X_{II}$, we cannot distinguish unambiguously between these two mechanisms on the basis of the present data.

The Influence of Some Additives on the Form II to Form I Crystal Transformation

The effect of four different additives on the crystal transformation rate of polybutene-1 was studied. These additives were mechanically blended with pure BR homopolymer as described previously. Three of the additives were commercially available chemical compounds which had previously been shown to act as nucleating agents for crystallization from the melt and the other one was isotactic polypropylene. Among the three chemical compounds, 1-naphtylacetamide was reported to be very effective in promoting the crystallization of polybutene-1 from the melt.[14] Sodium benzoate has frequently been used to enhance the crystallization of isotactic polypropylene but does not appear to be as effective as 1-naphtylacetamide for polybutene-1 crystallization.

TABLE VII
Time Dependence of the Phase Fractions of Polybutene-1 Tubular Blown Films

Time T	Form II fraction	Form I fraction	Crystalline fraction	Amorphous fraction
Sample: BR resin DDR = 1				
10 min	0.099	0.153	0.252	0.748
2 h	0.093	0.196	0.289	0.711
4 h	0.081	0.200	0.281	0.719
18 h	0.038	0.299	0.337	0.663
89 h	0.010	0.387	0.397	0.603
Sample: BR resin DDR = 3				
5 min	0.136	0.258	0.394	0.606
30 min	0.132	0.300	0.432	0.568
80 min	0.113	0.401	0.514	0.486
4 hr	0.063	0.525	0.588	0.412
7 h	0.048	0.541	0.589	0.411
16.5 h	0.023	0.573	0.596	0.404
22.5 h	0.014	0.604	0.618	0.382
Sample: BR resin DDR = 6				
30 min	0.110	0.406	0.516	0.484
1.5 h	0.080	0.517	0.597	0.403
3 h	0.045	0.548	0.593	0.407
5 h	0.034	0.607	0.641	0.359
11 h	0.016	0.634	0.650	0.350
22 h	0.011	0.640	0.651	0.349
Sample: DP resin DDR = 1				
10 min	0.169	0.197	0.366	0.634
1 h	0.147	0.287	0.434	0.566
3 h	0.099	0.320	0.419	0.581
7.5 h	0.053	0.394	0.447	0.553
18 h	0.028	0.521	0.549	0.451
28 h	0.023	0.500	0.523	0.477
52.5 h	0.013	0.550	0.563	0.437
Sample: DP resin DDR = 3				
20 min	0.185	0.194	0.379	0.621
40 min	0.168	0.218	0.386	0.614
2 h	0.130	0.322	0.452	0.548
5 h	0.079	0.432	0.511	0.489
8.5 h	0.051	0.480	0.531	0.469
20.5 h	0.025	0.532	0.557	0.443
36 h	0.015	0.544	0.559	0.441
Sample: DP resin DDR = 6				
5 min	0.259	0.422	0.681	0.319
15 min	0.234	0.470	0.704	0.296
1 h	0.153	0.552	0.705	0.295
2 h	0.088	0.732	0.820	0.180
3 h	0.046	0.801	0.847	0.153

The effectiveness of the present additives as nucleating agents for crystallization was tested by measuring their crystallization temperatures in a differential scanning calorimeter (DSC). The crystallization temperature of each sample was measured at a fixed cooling rate of 40°C/min. If a nucleating effect is present, we would expect to observe a higher crystallization temperature than for the unnucleated PBNO sample. The results shown

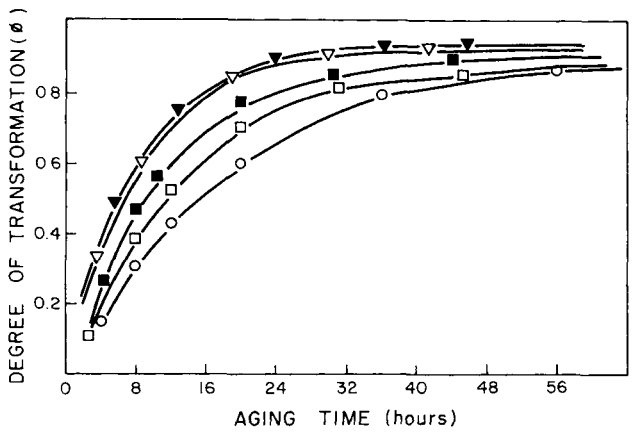

Fig. 12. (▼) PBN 4; (▽) PBN 3; (■) PBN 2; (□) PBN 1; (○) PBN 0. $T = 23$°C.

in Table II clearly show that polypropylene and 1-naphtylacetamide are effective nucleating agents in our samples. There seems to be little effect of sodium benzoate or stearic acid in the concentrations present.

In Figure 12 the effect of sodium benzoate (PBN1, PBN2) and isotactic polypropylene (PBN3, PBN4) on the phase transformation of polybutene-1 is compared against the BR homopolymer (PBNO). As may be seen, both additives are effective in promoting the transformation, but isotactic polypropylene has more effect at the concentrations used than sodium benzoate. Their effectiveness also depends on the concentration of the additive (wt %). It should be noted that isotactic polypropylene is present in rather high concentration (5%, 10%) in a mechanical blend.

In Figure 13 stearic acid (PBN8, PBN9) is found to be only slightly effective in promoting the crystal transformation at least at the concentrations used in this investigation. 1-Naphtylacetamide (PBN6, PBN7) which promotes the crystallization rate of polybutene-1 is not effective in promoting the crystal transformation. In fact, it appears that 1-naphtylacetamide actually retards the crystal transformation. From this, it can be

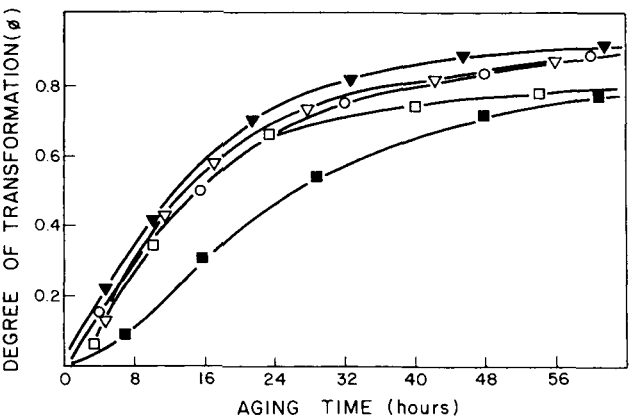

Fig. 13. (▼) PBN 9; (▽) PBN 8; (■) PBN 7; (□) PBN 6; (○) PBN 0. $T = 23$°C.

inferred that a nucleating agent which is effective in promoting the crystallization of polybutene-1 may not be effective in promoting the crystal transformation.

Isotactic polypropylene was most effective in promoting both the crystallization process and the crystal transformation of polybutene-1 among the several additives used. Isotactic polypropylene may be effective in promoting crystallization because it has higher melting point than polybutene-1. When a mechanical blend of polybutene-1 and polypropylene (PBN3, PBN4) is quenched from the melt state, polypropylene may crystallize first and act as a heterogeneous nucleating agent for the crystallization of form II. The fact that isotactic polypropylene is also active in promoting the crystal transformation of polybutene-1 might be attributable to the fact that polybutene-1 form I and polypropylene have the same helix structure (3_1). Conceivably, the polypropylene may produce some nuclei of form I directly from the melt, or at the interface between form II and polypropylene during the period immediately after the formation of form II. Another possible explanation is that the polypropylene acts as a plasticizer that enhances molecular mobility rather than as a nucleating agent for form I. Boor and Mitchell[21] examined this effect briefly at a series of temperatures. They found that polypropylene accelerated the transformation of form II to form I at aging temperatures near and above room temperature where nucleation should control, but had little effect at temperatures below room temperature where molecular mobility should control. It is thus likely that the effect is due to enhanced nucleation rather than enhanced molecular mobility.

In the present results there seems to be no definite relationship between effectiveness of an additive as a nucleating agent for crystallization and its effectiveness in promoting the phase transformation. It would seem, however, that this subject deserves additional study to elucidate the factors that control the effect of additives on the phase transformation rate.

INTERPRETATION AND DISCUSSION OF RESULTS

Analysis of Crystal Transformation Kinetics Using the Avrami Equation

Some previous investigators[3,6,9,10,28] have applied the Avrami equation to analyze the form II to form I phase transformation in polybutene-1. We follow that approach here. We assume as a first approximation that the degree of crystal transformation, ϕ, changes with time according to the equation

$$1 - \phi = \exp(-Kt^n) \tag{9}$$

where K is the rate constant for the transformation and n is the Avrami exponent. Taking the logarithm of this equation twice gives

$$\log \log[1/(1 - \phi)] = \text{const} + n \log t \tag{10}$$

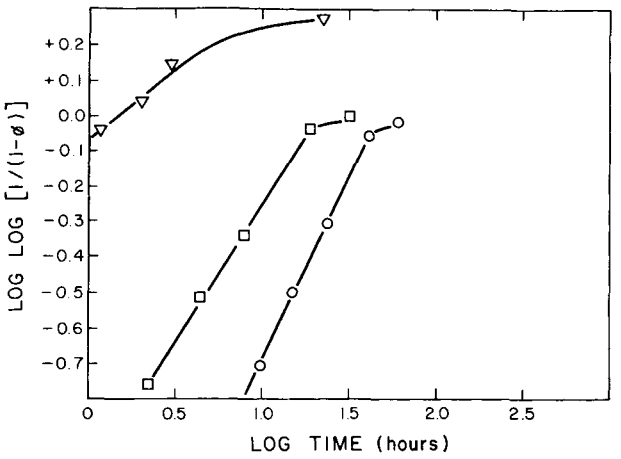

Fig. 14. (▽) 10% cold rolling; (□) 5% cold rolling; (○) no cold rolling. $T = 23$°C.

Thus the Avrami exponent was determined from the slope of a plot of log log $[1/(1 - \phi)]$ vs. log t. The rate constant K was computed from the value of n and the measured half-life of the transformation through

$$K = \ln 2/t_{1/2}^{n} \tag{11}$$

Figures 14–16 show typical plots according to eq. 10. The straight lines of all Avrami plots become gentle curves as the crystal transformation nears completion. This behavior is not uncommon when applying the Avrami analysis and may be due to a change of mechanism in the late stages of transformation. Values of n, K, and half-life are tabulated in Table VIII. The values of half-life and rate constant are consistent with the qualitative features of the transformation described previously. The n values correspond to the linear segment of the Avrami plots.

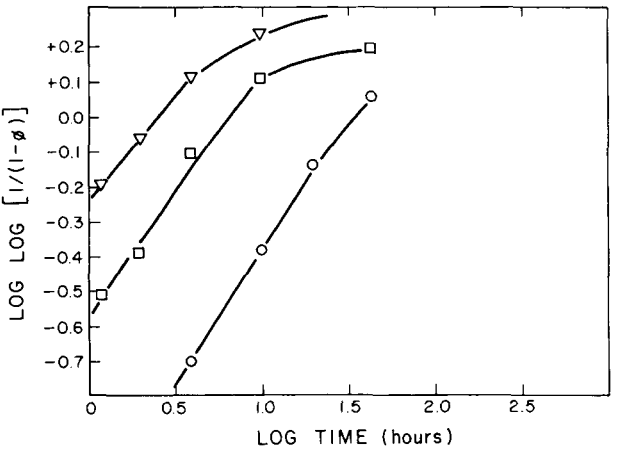

Fig. 15. (△) DDR = 6, $t = 55$ μm; (□) DDR = 3, $t = 110$ μm; (○) DDR = 1, $t = 390$ μm; $T = 23$°C, BUR = 1.

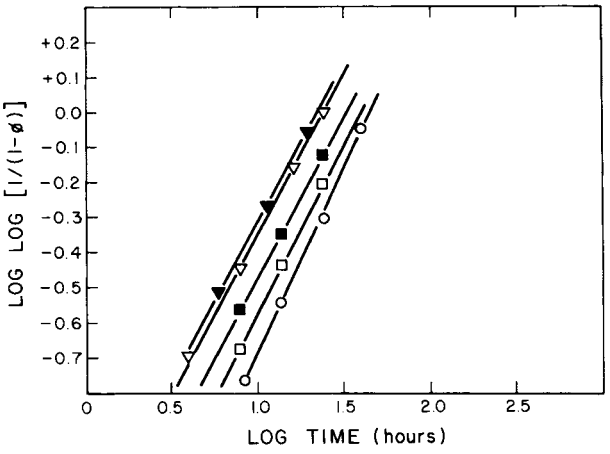

Fig. 16. (▼) PBN 4; (▽) PBN 3; (■) PBN 2; (□) PBN 1; (○) PBN 0. $T = 23°C$.

Table VIII shows that the undeformed compression molded samples with or without additives generally have Avrami exponents that are approximately unity (0.90–1.07). Exceptions are the DP resin ($n = 0.76$) and sample PBN7 ($n = 1.27$) which contains 0.5% 1-naphtylacetamide. It is not clear why these should differ from the other samples.

TABLE VIII
Results of Avrami Analysis of the Form II to Form I Phase Transformation in Polybutene-1

Compression-molded samples	Half-life $t_{½}$ (h)	Avrami exponent n	Rate constant $K \times 10^2$
PBN0	15	1.05	4.0
PBN1	11	0.96	6.9
PBN2	9	0.94	8.8
PBN3	7	0.93	11.3
PBN4	6	0.91	13.6
PBN6	15	1.07	38
PBN7	26	1.27	1.1
PBN8	14	0.90	6.4
PBN9	13	0.98	5.6
Molded and cold rolled			
BR-0% CR	15	1.05	4.0
BR-5% CR	4.4	0.79	21.5
BR-10% CR	< 0.5	0.38	> 100
BR-20% CR	< 0.1	0.27	> 500
DP-0% CR	2.0	0.76	40.9
DP-5% CR	< 1.0	0.66	69.3
DP-8% CR	< 0.5	0.25	> 100
Blown film samples			
BR,DDR = 1	6.0	0.74	18.4
BR,DDR = 3	1.2	0.69	61.1
BR,DDR = 6	< 0.5	0.59	> 100
DP,DDR = 1	< 0.5	0.39	> 100
DP,DDR = 3	< 0.5	0.39	> 100
DP,DDR = 6	< 0.1	0.32	> 500

The application of cold rolling or melt processing (film blowing) results in a decrease of the value of n.

Values of n near unity suggest that crystal form I nuclei spontaneously formed almost immediately after the polymer melt crystallizes into the crystal form II. The growth of the crystal form I nuclei occurs along only one direction, presumably the helix axis of the polymer chains as suggested by Geil et al.[28]

The Avrami exponents which are considerably less than unity cannot be fully explained at this time. It can only be guessed that cold rolling or melt processing may disturb the usual mechanism of the crystal transformation. The crystal transformation mechanism may change from one involving predetermined nucleation and one-dimensional growth in the absence of mechanical deformation to one or more deformation aided mechanisms.

Further understanding of the phase transformation requires a more complete accounting of the changes in the total crystallinity level during the transformation as well as the relative amount of form I and form II. A discussion of these aspects of the problem is presented in the next section.

Analysis of Crystal Transformation Combined with Secondary Crystallization

As described previously, the two phenomena of phase transformation and secondary crystallization take place simultaneously. There are two different routes by which this can occur. In the first case the amorphous phase could transform to form II which subsequently transforms to form I.

However, from a thermodynamic point of view it is just as reasonable that the amorphous phase transform directly to form I crystals. Thus, this mechanism must also be considered possible.

There are still other possible mechanisms for the secondary crystallization. Another important mechanism of the secondary crystallization might be the perfection of the imperfect crystals of forms II and I. Or, there may be some combination of these mechanisms. This makes the unabmiguous analysis of the secondary crystallization virtually impossible. Nevertheless, it would seem useful to examine some of these possibilities further. This is done here for the case of the compression molded sheets in the absence of further complication due cold working.

We assume that secondary crystallization may be described by

$$X_T = X_{II}^0 + k \log(t - t_0) \tag{12}$$

where X_{II}^0 is the initial crystallinity (assumed to be form II) at the time origin of secondary crystallization, t_0, and X_T is the total crystallinity of the sample. We also assume that the crystal transformation can be represented by the Avrami equation.

If we assume that the mechanism of the secondary crystallization is the crystallization of the amorphous phase into the crystal form II only, the relationships among X_I, X_{II}, and X_T would be the following equations:

$$X_T = X_{II}^0 + k \log(t - t_0) \tag{13}$$

$$X_{II} = X_T \exp(-Kt^n) \tag{14}$$

$$X_I = X_T \exp(-Kt^n)\,[\exp(Kt^n) - 1] \tag{15}$$

If the mechanism is assumed to be the transformation of the amorphous phase into the crystal form I only, the relationships among X_I, X_{II}, and X_T would be slightly different from the previous case:

$$X_T = X_{II}^0 + k \log(t - t_0) \tag{16}$$

$$X_{II} = X_{II}^0 \exp(-Kt^n) \tag{17}$$

$$X_I = X_{II}^0 \exp(-Kt^n)\,[\exp(Kt^n) - 1] + k \log(t - t_0) \tag{18}$$

These two extreme cases of possible mechanisms for the secondary crystallization were examined by calculating X_{II} and X_I according to the appropriate equations and comparing the theoretical estimates with the experimental data for the as-compression molded BR and DP resins. The values of Avrami exponent, n and rate constant K could be obtained from Table VIII. Variation of the total crystallinity X_T with time was used to evaluate k. With n, K, and k known, the above equations could be used to calculate the theoretical estimates of X_I and X_{II}. It was also assumed that the secondary crystallization and the crystal transformation of PB-1 takes place simultaneously, i.e., $t_0 = 0$. The initial crystallinity at the origin of the crystal transformation (X_{II}) was determined by extrapolation of the X_T vs. t plots.

In Figures 17 and 18 the experimental "crystallinity indexes" of crystal form II and crystal form I (X_{II}, X_I) for the compression-molded BR and DP resins are compared with their counterparts computed from eqs. (14)–(17). It is clear from both figures that the assumed mechanism of the transformation of the amorphous phase into the crystal form I directly fits better with the experimental values than does the assumed mechanism of the transformation of the amorphous phase into the crystal form II only. How-

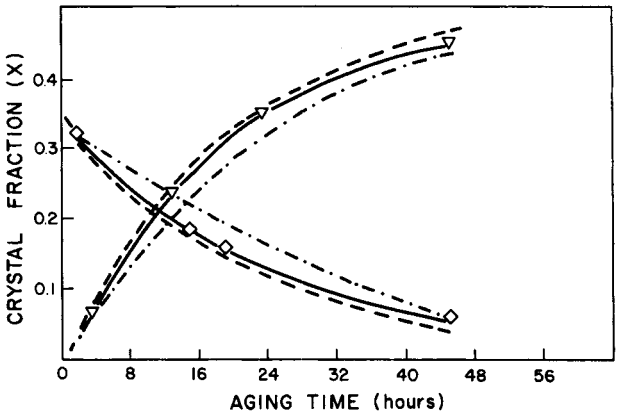

Fig. 17. BR 0%: (△) experimental X_{II}; (- - -) theor. X_{II} (am. → II); (- - -) theor. X_{II} (am. → I); (▽) experimental X_I; (——) theor. X_I (am. → II); (- - -) theor. X_I (am. → I).

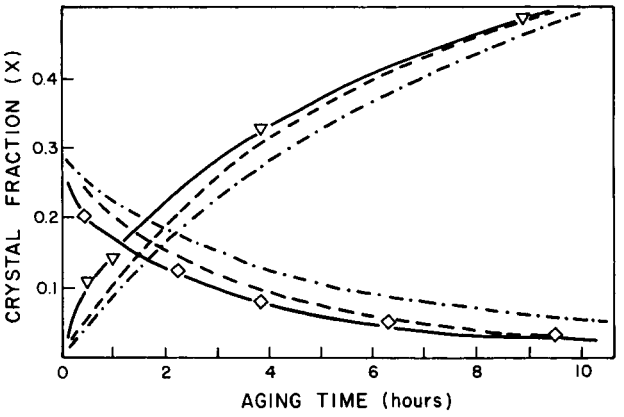

Fig. 18. (△) experimental X_{II}; (- · -) theor. X_{II} (am. → II); (- - -) theor. X_{II} (am. → I); (▽) experimental X_I; (- · -) theor. X_I (am. → II); (- - -) theor. X_I (am. → I).

ever, the fit for the latter mechanism is not so poor as to rule it out entirely, particularly in view of the fact that adjustments of the K and n parameters might produce still better fits. Nevertheless, the results suggest that the secondary crystallization may involve formation of form I directly from the supercooled amorphous phase. These results seem to be consistent with the data of Burns and Turnbull,[30] who found that crystal form I would nucleate (heterogeneously) directly from the melt at very large supercooling.

Discussion of the Mechanism of the Form II to Form I Phase Transformation

The kinetics of the transformation of modification II (tetragonal) to modification I (hexagonal) have been studied by the Avrami analysis giving the Avrami exponent n. The Avrami exponent was found to approach unity at room temperature for unstressed BR resin (including the nucleated samples, PBN1–PBN9). The fact that $n \simeq 1$ may mean that the transformation mechanism involves instantaneous (predetermined) nucleus formation and a one-dimensional growth process. Oda et al.[12] also found the value of Avrami exponent, $n = 1$, at room temperature, arguing that the transformation mechanism is a nonuniform nucleus formation and its growth is first order. Geil et al.[28] obtained $n \simeq 0.9$ at room temperature. They suggested that the nuclei form almost simultaneously throughout the sample and the transformation takes place along the individual ribbons which constitute the spherulites. The first order growth of hexagonal crystal may be explained on the basis that the predetermined nuclei of crystal form I grow only in the direction of the helix axis (c-axis) of crystal form II and the growth in each crystal ribbon is independent of that in other ribbons.

As mentioned before, the Avrami exponents of nucleated materials (PBN1–PBN9) nearly all approach unity (Table VIII). It seems that these additives act as heterogeneous nucleating agents for the crystal form I and thus increase the nucleation rates of the crystal form I. This will result in the increase of the crystal transformation rates K (Table VIII). The fact that $n \simeq 1$ indicates that these additives do not change the basic mechanism

of transformation mentioned in the above paragraph. That is, crystal form I nuclei formed on the heterogeneous nucleating agents also grow only in the helix axis direction of crystal form II.

It was suggested above that the enhancement of transformation rate by small rolling reductions was the result of the stresses applied rather than the orientation produced. Actually, the crystal form I helix (3_1) is a more extended chain than the crystal form II helix (11_3).[3-5,19] The application of stress or strain may thus mechanically assist the crystal transformation. Geil et al.[28] maintained that the driving force for propagation of the crystal transformation is the interfacial strain energy between the form II matrix and the growing form I during the helical axis expansion. It seems that this interfacial strain energy may be assisted during cold rolling by the forced helical axis expansion ($11_3 \rightarrow 3_1$).

Other forms of mechanical deformation such as applied tension should also lead to enhanced transformation rates, and this has indeed been observed by previous investigators.[6,11,18] It is of interest to note that the level of enhancement observed in the present study by small amounts of cold rolling is greater than that reported by Oda for similar amounts of tensile deformation.[9] This would seem to imply that the greater amount of redundant work performed on the sample to achieve the shape change by rolling has a significant effect on the transformation rate.

The tubular blown films of polybutene-1 were studied morphologically by small angle light scattering (SALS). The spherulitic features of hardly-oriented product (DDR = 1) were found to change into the "sheaflike" structures of highly oriented product (DDR = 6). The "sheaflike" structure of polybutene-1 blown films was previously reported by Hashimoto et al.[25] Based on electron microscopy they associated the "sheaflike" structure with a row-nucleated structure of folded chain lamellae. The blown film also exhibited substantial levels of orientation consistent with the "sheaflike" structure. Samples containing frozen-in orientation generally also contain frozen-in stresses. These stresses would be exerted primarily along the machine direction and they would increase with DDR. Since both the frozen-in stress and chain orientation parallel to the machine direction would increase with DDR, it can be argued that the frozen-in stress assists the phase transformation in melt oriented samples. Therefore, according to this mechanism, it can be said that orientation itself does not accelerate the crystal transformation but helps to get the appropriate level of the residual stress along the chain axes to accelerate the transformation.

SUMMARY AND CONCLUSIONS

The form II to form I phase transformation in polybutene-1 was studied at room temperature using density and wide angle X-ray scattering techniques. The effects on the rate of phase transformation of deformation by cold rolling, orientation produced by melt processing (film blowing), and certain additives blended with the homopolymer were examined. A new technique to calculate the approximate fractions of form I, form II, and amorphous phase present in a given sample was devised based on the com-

bination of density and wide angle X-ray diffraction measurements. The studies resulted in the following conclusions.

1. Cold rolling is a very effective method of enhancing the form II to form I phase transformation in polybutene-1. The introduction of small levels of solid state strain by cold rolling produced immediate partial transformation to form I followed by further transformation which proceeded at enhanced rates.

2. The rate of crystal transformation, K, increases with the increase of melt orientation introduced by the tubular film blowing process.

3. Isotactic polypropylene is very effective in promoting the crystal transformation of isotactic polybutene-1.

4. A nucleating agent which is effective in promoting the crystallization of polybutene-1 may not be effective in promoting the crystal transformation (in the same concentration range).

5. The fact that $n \simeq 1$ for unstressed samples may indicate that the basic mechanism of the crystal transformation is the one-dimensional growth of instantaneous (predetermined) nuclei.

6. Additives do not disturb the basic mechanism of the crystal transformation but seem to accelerate the crystal transformation by increasing the number of predetermined nuclei of crystal form I.

7. Cold rolling or melt orientation produced by film blowing results in Avrami exponents substantially below unity. The significance of these low values is not yet clear.

8. A comparison of the experimental data and an analytical description of the transformation including the secondary crystallization suggests that crystal form I may form directly from the supercooled amorphous material remaining after an ice-water quench as well as from the crystalline form II material obtained during the quench.

9. The orientation produced by small amounts of plastic deformation by cold rolling is very low compared to orientation produced by the film blowing technique, but cold rolling is more effective in enhancing the phase transformation. This suggests that the enhancement of crystal transformation by cold rolling is primarily the result of the stresses or strains applied rather than the orientation produced.

10. It appears that the acceleration of the crystal transformation of tubular blown films may be the result of the effective uniform distribution of the residual shrinkage stress induced by the deformation of melt rather than the orientation produced, per se. However, additional research is needed in order to fully establish this point.

The authors are indebted to Shell Development Company for supplying the resins used in this research. We also wish to acknowledge several useful discussions of the data analysis with Dr. K Koyama. We also wish to thank the National Science Foundation for partial support of this research.

References

1. G. Natta, P. Pino, P. Corradini, F. Danusso, E. Mantica, G. Mazzanti, and G. Moraglio, *J. Am. Chem. Soc.*, **77**, 1708 (1955).

2. G. Natta, *Angew. Makromol. Chem.*, **16**, 213 (1955).

3. J. Boor, Jr. and J. C. Mitchell, *J. Polym. Sci.*, **1**, (Part A), 59 (1963).
4. V. F. Holland and R. L. Miller, *J. Appl. Phys.*, **35** (11), 241 (1964).
5. G. Cojazzi, V. Malta, G. Celotti, and R. Zannetti, *Macromol. Chem.*, **177**, 915 (1976).
6. T. Asada, J. Sasada, and S. Onogi, *Polym. J.*, **3**, 350 (1972).
7. G. Goldbach, *Angew. Makromol. Chem.*, **29/30**, 213 (1973).
8. S. Y. Choi, J. P. Rakus, and J. L. O'Toole, *Polym. Sci Eng.*, **6**, 349 (1966).
9. T. Oda, M. Maeda, S Hibi, and S. Watanabe, *Kobunshi Ronbunshi*, **31**, 129 (1974).
10. J. Powers, J. D. Hoffman, J. J. Weeks, and F. A. Quinn, Jr., *J. Res. Natl. Bur. Stand.*, **69A**, 335 (1965).
11. G. Goldbach, *Angew. Makromol. Chem.*, **39**, 175 (1974).
12. T. Oda, M. Maeda, S. Hibi, and S. Watanabe, *Kobunshi Ronbunshu, Engl. Ed.*, **3**(2), 1249 (1974).
13. T. W. Haas and B. Maxwell, *Polym. Eng. Sci.*, **9**, 225 (1969).
14. A. M. Chatterjee, U.S. Pat. 4,322,503, March 30, 1982; U.S. Pat., 4,320,209, May 16, 1982.
15. A. M. Chatterjee, F. P. Price, and S. Newman, *J. Polym. Sci., Polym. Phys. Ed.*, **13**, 2369 (1975).
16. M. Cortazar, C. Sarasola, and G. M. Guzman, *Eur. Polym. J.*, **18**, 439 (1982).
17. G. Natta, P. Corradini, and I. W. Bassi, *Nuovo Cimento Suppl.*, **15**, 52 (1960).
18. A. Tanaka, N. Sugimoto, T. Asada, and S. Onogi, *Polym. J.*, **7**, 529 (1975).
19. A. T. Jones, *Polymer*, **7**, 23 (1966).
20. Y. D. Lee and J. E. Spruiell, SPE ANTEC Conference Proceedings, 1984, Vol. XXX, New Orleans, LA (1984).
21. J. Boor, Jr., and J. C. Mitchell, *J. Polym. Sci.*, **62**, 870 (1962).
22. A. M. Chatterjee, *Mod. Plast. Ency.*, (Feb), 49 (1983).
23. F. L. Binsbergen, *Polymer*, **11**, 253 (1970).
24. J. Bheda and J. E. Spruiell, SPE ANTEC Conference Proceedings, 1984, Vol. XXX, (1984).
25. T. Hashimoto, A. Todo, Y. Murakami, and H. Kawai, *J. Polym. Sci.*, **15**, 501 (1977).
26. A. Keller and M. J. Machin, *J. Macromol. Sci. Phys.*, **B1**(1), 41 (1967).
27. J. E. Spruiell and J. L. White, *Polym. Eng. Sci.*, **15**, 666 (1975).
28. P. H. Geil, Y. C. Yang, K. W. Chan, C. C. Hsu and A. Agarwal, SPE ANTEC Conference Proceedings, (1983), Vol. XXIX, p. 404.
29. B. H. Clampitt and R. H. Hughes, *J. Polym. Sci. (Part C)*, **6**, 43 (1964).
30. J. R. Burns and D. Turnbull, *J. Polym. Sci.*, **6**, 775 (1968).

Received February 29, 1984
Accepted December 11, 1984